Editors' Suggestion

Disordered flat bands on the kagome lattice

Thomas Bilitewski and Roderich Moessner
Max-Planck-Institut für Physik komplexer Systeme, Nöthnitzer Strasse 38, Dresden 01187, Germany

(Received 27 September 2018; published 5 December 2018)

We study two models of correlated bond and site disorder on the kagome lattice considering both translationally invariant and completely disordered systems. The models are shown to exhibit a perfectly flat ground-state band in the presence of disorder for which we provide exact analytic solutions. Whereas in one model the flat band remains gapped and touches the dispersive band, the other model has a finite gap, demonstrating that the band touching is not protected by topology alone. Our model also displays fully saturated ferromagnetic ground states in the presence of repulsive interactions, an example of disordered flat band ferromagnetism.

DOI: 10.1103/PhysRevB.98.235109

I. INTRODUCTION

The physics of flat bands has generated considerable excitement over the years [1–3]. In a flat band, the kinetic energy is completely suppressed; thus, transport is hindered by a vanishing group velocity, and any kind of interaction is nonperturbative in nature and can mix the extensive number of degenerate states in the flat band, with the potential to create complex many-body states and phenomena. One well-known example of this mechanism at work is the fractional quantum Hall effect, where interactions induce highly nontrivial behavior of the electrons in the degenerate Landau levels of a magnetic field.

Thus, flat band systems are well suited for producing unconventional phenomena [2,4,5]. For both fermions and bosons, they allow us to realize the fractional quantum hall effect in absence of a magnetic field [6–9], i.e., fractional Chern insulators, and at potentially high temperatures [10]. Other contexts include high-temperature superconductivity [11,12], Wigner crystallization [13,14], realizing higher-spin analogs of Weyl-fermions [15], bands with chiral character [16], lattice supersolids [17], fractal geometries [18], magnets with dipolar interactions [19], and Floquet physics [20,21]. Flat bands of magnons also play a crucial role in determining the behavior of quantum magnets in magnetic fields [22–25].

Interest in flat band physics is not restricted to the presence of interactions, but also extends to their response to disorder, as the flat band states can turn out to be critical displaying multifractality [26], or unconventional localization behavior [27–29]. They also appear in purely classical mechanical systems [30], and in the field of photonics [31,32]. Quite recently, flat bands have been experimentally demonstrated in a realistic kagome material [33] as well as in optical lattices [34].

In this work we consider noninteracting nearest-neighbor hopping models on the kagome lattice with correlated bond and site-disorder, as illustrated in Fig. 1. The simple nearest-neighbor hopping model on the kagome lattice is known to host a degenerate flat band [35–39] with a quadratic band touching point believed to be topologically protected [40]. However, in interacting many-body physics it is often preferable to work with a gapped flat band to protect it from "Landau-level mixing," i.e., from interactions with the dispersive bands.

Here, we explicitly construct a gapped flat band on the kagome lattice. The simplest setting in which it appears contains modulated bond and site disorder, both in the presence of translational symmetry (where one can speak of a band) and in the absence of it, i.e., in the presence of random disorder, where one may still identify an extensive manifold of degenerate states. In fact, we find that a local perturbation to the Hamiltonian can open a gap above the flat band. This indicates that the band touching is protected not just by topology but requires also symmetry.

We obtain exact solutions for the flat band s tates of all of these models, facilitating a clear interpretation of why the chosen type of correlated site-bond disorder does not lift the extensive degeneracy of the flat band, and providing insight into the stability of the flat bands and the protection of the quadratic band-touching point. Our study also adds an example where compactly localized Wannier states can be explicitly constructed for a disordered flat band model.

Our treatment extends previous observations on the flat band in kagome, such as the observed stability of the flat band and band-touching points to breathing anisotropy [41], and opens up interesting perspectives: We show how to selectively gap out the flat band, or the Dirac cones, or all bands. Thus, our results reinforce the role of the kagome lattice as a platform for the study of topological physics and flat band physics in general, in particular the physics of perturbations and disorder in flat bands.

II. MODEL

We study noninteracting particles on the kagome lattice:

$$\mathcal{H} = \sum_{\langle i,j\rangle}(t_{ij}\hat{c}_i^\dagger\hat{c}_j + \text{c.c.}) + \sum_i \mu_i \hat{n}_i, \qquad (1)$$

with nearest-neighbor (complex) hoppings t_{ij} between sites i, j and site-dependent chemical potentials μ_i at site i. In the models we consider that μ_i is given as a function of the couplings t_{ij}. The specific correlation between the hopping

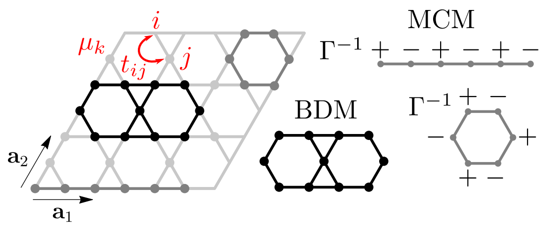

FIG. 1. Kagome lattice with lattice vectors a_1 and a_2. Shown is a finite-size lattice with $L_x = L_y = 3$; opposite edges are identified for periodic boundary conditions. The model contains site-dependent nearest-neighbor tunnelings t_{ij} and chemical potentials μ_k. The highlighted sites correspond to a zero-energy flat band state of the MCM, hexagon, and system-spanning loop (dark gray) or the BDM, double hexagon (black).

and potential terms is motivated by a connection to bond-disordered Heisenberg models [42] where it naturally arises via an exact rewriting of the Hamiltonian.

The Hamiltonian can be compactly written via its matrix elements H_{ij} as $\mathcal{H} = \sum_{ij} c_i^\dagger H_{ij} c_j$. Noting that this only connects nearest neighbors, and that every nearest-neighbor pair belongs either to an up or down triangle of the kagome lattice, we rewrite the Hamiltonian in the following way:

$$\mathcal{H} = \mathcal{H}^\triangle + \mathcal{H}^\triangledown \tag{2}$$

$$H_{ij}^{\triangle/\triangledown} = \begin{cases} \bar{\gamma}_i^{\triangle/\triangledown}\gamma_j^{\triangle/\triangledown} + |\gamma_i^{\triangle/\triangledown}|^2\delta_{ij}, & \text{for } i,j \in \alpha, \\ 0, & \text{otherwise}, \end{cases} \tag{3}$$

where we first split it into its contribution on the up and down triangles, and then define all couplings within a triangle α via site and triangle dependent (complex) factors $\gamma_i^{\triangle/\triangledown}$.

This form makes the correlation between the hoppings and chemical potentials explicit. Specifically, we have $t_{ij} = \bar{\gamma}_i^\alpha \gamma_j^\alpha$ for sites i, j in the triangle α and $\mu_i = |\gamma_i^\triangle|^2 + |\gamma_i^\triangledown|^2$. In the presence of lattice-inversion symmetry $\mathcal{H}^\triangle = \mathcal{H}^\triangledown$ and these factors become solely site dependent. We will refer to the model with lattice inversion symmetry as the maximal Coulomb model (MCM), and with broken lattice inversion symmetry as the bond-disordered model (BDM).

This also allows us to make an insightful connection to the Hamiltonian of the nondisordered model; essentially the disordered model can be understood as a rescaling of the clean model by the γ factors. Using that the Hamiltonian is fully specified by its matrix elements H_{ij}, we can further split them as a product of three matrices as

$$H^{\triangle/\triangledown} = \bar{\Gamma}^{\triangle/\triangledown} H_0^{\triangle/\triangledown} \Gamma^{\triangle/\triangledown} \tag{4}$$

with $\Gamma_{ij}^{\triangle/\triangledown} = \delta_{ij}\gamma_i^{\triangle/\triangledown}$, a diagonal matrix containing the scaling factors, and H_0 the matrix of the clean system with $\gamma_i^\alpha \equiv 1$, describing the nearest-neighbor hopping on the kagome lattice.

Making use of the form $\mathcal{H} = \sum_{ij} c_i^\dagger H_{ij} c_j$ the action of the Hamiltonian on single-particle states $|\Psi\rangle = \sum_i \psi_i c_i^\dagger |\text{vac}\rangle$ is simply

$$\mathcal{H}|\Psi\rangle = \sum_i H_{ik}\psi_k c_i^\dagger|\text{vac}\rangle = \sum_i (H\psi)_i c_i^\dagger |\text{vac}\rangle. \tag{5}$$

From this we obtain the expectation value as

$$\langle\Psi|\mathcal{H}|\Psi\rangle = \sum_{ij}\bar{\psi}_i H_{ij}\psi_j = \sum_\alpha \left|\sum_{i\in\alpha}\gamma_i^\alpha\psi_i\right|^2 = \sum_\alpha |\psi_\alpha|^2, \tag{6}$$

where in the second equality we used the explicit form of the Hamiltonian, Eq. (3), which splits into a sum over triangles α, and in the last equality defined the sum of scaled amplitudes within a triangle $\psi_\alpha = \sum_{i\in\alpha}\gamma_i^\alpha\psi_i$.

Thus, exact zero modes are states with $\psi_\alpha = 0$ on all triangles α. This condition is typically referred to as a ground-state constraint in the theory of frustrated magnets and is intimately connected to height mappings and emergent gauge theory descriptions of the ground-state phase. For spins the condition $\psi_\alpha = 0$ is more stringent and can only be fulfilled for not too disparate bond values due to the unit length constraint which is found to lead to a phase transition of the model. In contrast, here it can be fulfilled for arbitrary choices.

III. CONSTRUCTION OF FLAT BAND STATES

A. Exact mapping of flat band for the MCM

The clean system is known to host an exactly flat band at $E = 0$ which touches the dispersive band at $q = 0$ [40].

In the nondisordered model ($\gamma_i^\alpha = 1$), the ground-state condition $\psi_\alpha = \sum_{i\in\alpha}\psi_i = 0$ reduces to the simple sum of amplitudes in every triangle vanishing. It is easy to check that the states illustrated in Fig. 1, a hexagon loop with alternating $+, -$, and a system-spanning loop with alternating $+, -$ amplitudes, satisfy this, and (less trivially) that these yield $N_s/3 + 1$ linearly independent zero-energy states. Since the kagome lattice has three sites in the unit cell and thus three bands, finding $N_s/3 + 1$ states at the same energy then also implies the band touching.

For the MCM all these zero modes of the clean system can be mapped to zero modes of the disordered model via

$$\Psi_{\text{MCM}}^{\text{FB}} = \Gamma^{-1}\Psi_0^{\text{FB}}, \tag{7}$$

which follows directly from $H^\triangle = H^\triangledown$ in the MCM together with Eqs. (4) and (5), e.g., the observation that the disordered model can be understood as a rescaling of the clean model. Thus, we obtain an exactly flat band at $E = 0$. This further implies that the band touching point is preserved as well.

The flat band states of the MCM can therefore be characterized the same way as in the clean system [40]: the MCM (a) $N_s/3 + 1$ zero modes, (b) of which $(N_s/3 - 1)$ can be chosen as linearly independent localized hexagon loop modes and 2 as system-spanning delocalized loops (both types arising via the mapping from the zero modes of the clean system), and (c) the flat band is gapless touching the dispersive band. The two different types of states are schematically illustrated in Fig. 1.

We emphasize that this is completely independent of the specifics of γ_i, e.g., it holds true for translationally invariant, completely disordered, positive, negative, and sign-changing, and real or complex choices. In fact, it holds true for a slightly more general model, where $\Gamma^\triangle = c\,\Gamma^\triangledown$ which in particular includes the model with breathing anisotropy.

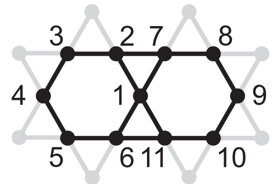

FIG. 2. A double hexagon of the kagome lattice. The wave function of a BDM zero energy state is localized on the black sites. Note that the state occupies 11 sites, and is part of 10 triangles, thus, there are 11 degrees of freedom and 10 constraints, in addition to the wave-function normalization, implying that there is a unique solution for such a localized state.

B. Construction of flat band for BDM

We note that such a mapping is not possible for the BDM where Γ differs nontrivially between up and down triangles. Thus, it is not immediately obvious that the BDM should host an extensively degenerate ground-state band and if so whether the band-touching point is preserved.

We first summarize the findings and then provide a construction of the flat band states. We find that (a) the BDM has $N_s/3$ exact zero modes/flat band, (b) the flat band states states can all be localized, and (c) the flat band is generically gapped.

We emphasize the last point, stating that it is possible to maintain the flatness of the band while gapping it from the dispersive bands in contrast to the claimed topological protection [40]. We will analytically show this in the next section for the translationally invariant model, and provide numerical evidence for disordered systems. In fact, it is sufficient to break inversion symmetry by changing a single coupling $\gamma_i^\triangle$ to create a gap to the flat band.

We now explicitly construct the $N_s/3$ linearly independent localized states forming the degenerate flat band. To do so, we consider a double hexagon of the kagome lattice shown with our conventions for the site labels in Fig. 2. We note that such a state occupies 11 sites and these sites are part of ten triangles of the kagome lattice. Each triangle contributes one scalar constraint $\Psi_\alpha = 0$, in addition to one normalization constraint, thus we might expect a unique solution on every hexagon pair.

The resulting linear system of equations can be solved explicitly [see the Supplemental Material (SM) [43]], and the wave-function amplitudes may be written as a function of the coupling terms γ_i^α as $\Psi_i = \Psi_1 f_i(\gamma_i^\alpha)/D(\gamma_i^\alpha)$. This solution is only valid if the determinant D given by

$$\Delta = \gamma_3^\triangledown\gamma_5^\triangledown\gamma_7^\triangledown\gamma_9^\triangledown\gamma_{11}^\triangledown\gamma_2^\triangle\gamma_4^\triangle\gamma_6^\triangle\gamma_8^\triangle\gamma_{10}^\triangle - (\triangledown \leftrightarrow \triangle), \tag{8}$$

is nonzero. This manifestly vanishes in the presence of inversion symmetry ($\gamma^\triangle = \gamma^\triangledown$), but is nonzero if inversion symmetry is broken ($\gamma^\triangle \neq \gamma^\triangledown$). Therefore, in the BDM there is a unique localized state on every double hexagon.

We have checked (numerically) that taking L^2 such double hexagons tiling the full kagome lattice does yield L^2 independent states, thus providing a full basis for the zero-energy states of the BDM, in contrast to the MCM and the clean system which requires the system spanning loop states [40].

It is also easy to show that no such solution for a localized state is possible on a single heaxagon (see the Supplemental Material [43]), thus, proving that these found states indeed form a maximally localized basis of the flat band manifold.

Typically, in the presence of interactions the size of the maximally localized basis states strongly affects the behavior of the model, and here we find that this size doubles in the presence of infinitesimal disorder. In fact, the existence of a compactly localized basis for flat bands is an open question of research with relations to the topology of the corresponding Bloch bands [44–46].

IV. GAPPED FLAT BANDS

It remains to show that the BDM flat band states are indeed gapped and do not touch the dispersive bands, which we will show in the next sections both for translationally invariant and generic disordered models.

A. Translationally invariant systems

We begin by considering translationally invariant systems with real couplings. In that case the model has six (three) free parameters $\gamma_{A,B,C}^{\triangle/\triangledown}$ for BDM (MCM), e.g., the couplings on the three sites (A,B,C) in a triangle of the kagome lattice, with different couplings on the up and down triangle for the BDM model.

In this case, one can analyze the model in momentum space, and analytical results can be obtained (see the SM [43]). We find that for every q there is exactly one zero mode, i.e., we find a flat band at $E = 0$ for both the BDM and MCM as anticipated from the construction of the zero modes above. Importantly, this allows us to obtain an analytic expression for the gap of the BDM, thus proving our claim that the BDM flat band can indeed be gapped.

We will consider illustrative examples for the gap below; please see the Supplemental Material [43] for the general expression of the gap. As the simplest model consider just $\gamma_A^\triangle \neq 1$, then the gap scales as

$$\Delta_{\text{gap}} = \tfrac{1}{2}\left(5 + {\gamma_A^\triangle}^2 - \sqrt{\left({\gamma_A^\triangle}^2 + 1\right)^2 + 16\gamma_A^\triangle + 16}\right) \tag{9}$$

showing a quadratic scaling for small deviations away from the homogeneous system.

A more symmetric arrangement can be obtained by considering $\gamma_A^\triangle = \frac{1}{\gamma_A^\triangledown} = \gamma_B^\triangledown = \frac{1}{\gamma_B^\triangle} = x$, which yields the gap to the flat band as

$$\Delta_{\text{gap}} = x^2 + x^{-2} - 2. \tag{10}$$

We note that this allows us to cleanly separate the flat band by an (arbitrarily) large gap from all dispersive bands, making the kagome lattice a prime platform to study physics in flat bands.

We show dispersion relations along high-symmetry lines in the Brillouin zone for the clean model, the MCM, and the BDM in Fig. 3. We emphasize that clearly both models retain an exactly flat band at $E = 0$. As discussed above the MCM always retains the band-touching point at $q = 0$ (Γ point), but the Dirac points can be gapped for large perturbations (not shown).

In contrast in the BDM, the flat band is always gapped as seen in the lower panel of Fig. 3, already for infinitesimal changes in the couplings. Just changing a single coupling

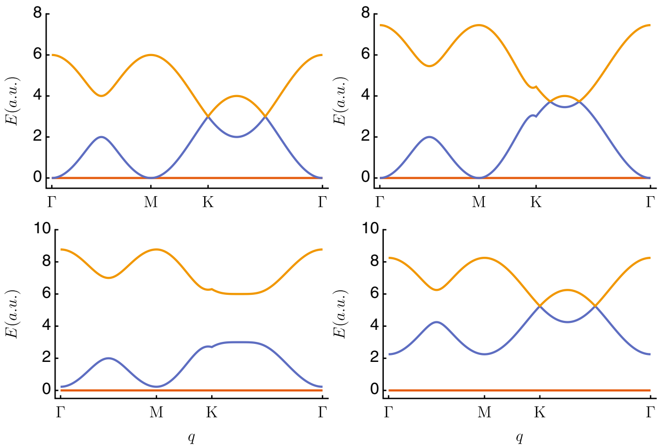

FIG. 3. Dispersion along high-symmetry lines in the Brillouin zone. From top left to bottom right: clean system, MCM with $\gamma_A = \gamma_A^{\triangle} = \gamma_A^{\nabla} < \sqrt{2}$, BDM with $\gamma_A = 2$, and BDM with $\gamma_A^{\triangle} = \frac{1}{\gamma_A^{\nabla}} = \gamma_B^{\nabla} = \frac{1}{\gamma_B^{\triangle}} = 0.5$.

generically gaps both the flat band and the Dirac points (lower left panel). For the symmetric choice described above, the flat band is gapped, but the Dirac points remain gapless (lower right panel).

In summary, we have shown that we can selectively gap out the flat bands and keep the Dirac cones or gap out the Dirac cones, but keep the quadratic band touching point, or gap out all bands.

B. Local perturbation

Before considering fully disordered models it is insightful to understand the effect of a local perturbation to the system. For a topologically protected band crossing one would expect the resulting gap to scale to zero exponentially in system size.

We modify the Hamiltonian locally by changing a single coupling $\gamma^{\triangle}$ affecting one site potential μ and two tunnel couplings t. As a result, in Fig. 4(a) we observe a linear decrease of the gap with inverse number of sites $\sim N_s^{-1}$,

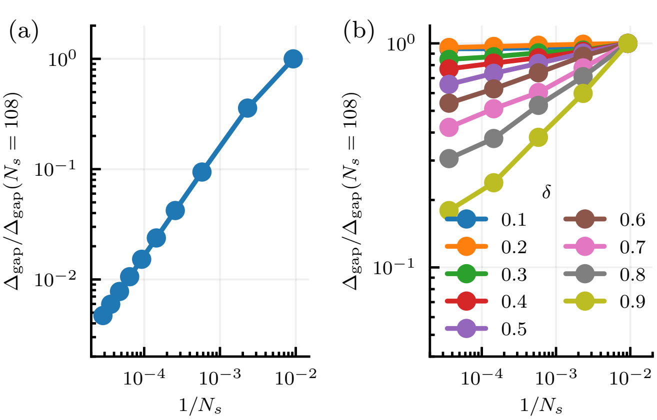

FIG. 4. (a) Gap of the flat band in presence of a local perturbation vs inverse number of sites N_s on a log-log scale showing a linear scaling with inverse number of sites $\sim N_s^{-1}$. (b) Gap of the flat band for the fully disordered system vs inverse number of sites for different disorder strengths δ.

consistent with the gap closing in the thermodynamic limit. However, the decay is clearly not exponential as would be expected for a topologically protected degeneracy.

C. Disordered systems

Next, we consider fully disordered models with random choices for $\gamma_i^{\triangle/\nabla}$. As an example we consider a box-uniform distribution $\gamma \in [1-\delta, 1+\delta]$. However, we emphasize that this specific choice is not relevant and the conclusions hold true for any generic disorder distribution.

The gap to the flat band versus inverse system size for a range of values of δ is shown in Fig. 4(b). It extrapolates to a finite value in the thermodynamic limit for $\delta < 1$, and scales as δ^2 for small disorder strengths. Thus, we conclude that disorder of this type gaps out the flat band, even for infinitesimal disorder strength.

We also note in passing that the finite gap implies that the projector into the flat band decays exponentially for the BDM model, but decays algebraically for the gapless MCM.

D. Flat band ferromagnetism in a disordered model

Flat bands are known to host ferromagnetic phases in the presence of repulsive interactions [35–39,47]. The presence of a gap to the flat band in our model ensures that the many-body ground state at filling $n = 1/6$ is the unique fully saturated ferromagnetic state.

To see this in our model of disordered flat bands, we consider a fermionic version with repulsive Hubbard interactions,

$$\mathcal{H} = \sum_{\langle i,j\rangle,\sigma} (t_{ij}\hat{c}_{i\sigma}^{\dagger}\hat{c}_{j\sigma} + \text{c.c.}) + \sum_i \mu_i \hat{n}_i + U\sum_i n_{\uparrow}n_{\downarrow}; \quad (11)$$

for spin-1/2 fermions, $n_i = n_{i\uparrow} + n_{i\downarrow}$, t_{ij} and μ_i are chosen as above, and we consider the BDM to have a flat gapped noninteracting band.

Since for $U > 0$ the interaction term is positive, and the kinetic energy is positive-definite by construction, many-body states with $E = 0$ are necessarily ground states.

One ground state is easily obtained by filling the noninteracting flat band completely with polarized spins which do not interact. Thus, we have at filling $n = 1/6$ a ferromagnetic ground state with maximal spin $S = L^2/2$, with the full $2S(2S+1)$ degeneracy due to the SU(2) symmetry of the model. The main question to obtain ferromagnetism is whether this ground state is unique, or if there are additional nonmagnetic states as well. Here, it turns out that the ground state is gapped, since the noninteracting band structure has a finite gap for the BDM.

We performed exact diagonalization of the Hubbard model, Eq. (11), on small finite-size kagome clusters (2×2, 2×3) to confirm that the ground state is indeed of the described form.

Finally, due to the presence of a spectral gap, we expect the ferromagnetism to be stable to finite perturbations and fluctuations in the particle number. Indeed, ferromagnetism is expected to be enhanced compared to the usual kagome case, since the localized noninteracting states now contain two hexagons.

V. OUTLOOK

Demonstrating that the flat bands of the kagome lattice can be gapped opens up the kagome lattice as a prime platform for the clean, i.e., isolated from the dispersive bands by an arbitrarily large gap, study of topological and more general flat band phenomena.

In addition, the presence of a flat band in a disordered model is highly nontrivial and of general interest even if it requires fine-tuning between the hopping and site-potential terms.

In terms of realizations of the specific type of couplings, we recall that this model is naturally realized in the large-N limit [48,49] of a classical nearest-neighbor bond-disordered Heisenberg (anti)ferromagnet, where the correlation between site and bond disorder arises from the spin length constraint. In other settings it is unlikely that bond- and site-disorder is correlated in the required way, thus, the system would need to be specifically designed. In this case we envision that it would be considerably easier to realize the translationally invariant model reducing the required number of parameters that have to be tuned. (For the minimal model we would require tuning one site potential and two tunneling couplings in each unit cell.) This might be feasible in cold-gas setups where control over individual sites and bonds is possible by the use of quantum gas microscopes.

In terms of topological properties of the flat band, we note that fluxes in the MCM model are trivial by construction (since they can be removed by a unitary gauge transformation). The BDM model in contrast supports nontrivial fluxes along the hexagon loops of the lattice. However, since in the BDM model all states of the flat band can be chosen localized, the noninteracting model is necessarily topologically trivial [50].

Our model also presents a natural realization of flat band ferromagnetism on the kagome lattice, where the gap of the single-particle spectrum results in a unique gapped fully saturated ferromagnetic many-body state in the presence of repulsive on-site interactions. We reserve the further discussion of interacting many-body phases in the gapped flat band and the effects on the magnon bands of magnets for future work.

It might also be interesting to explore the effect of longer-range interactions on the flat bands of this model which have recently been found to be remarkably stable for the nondisordered model [19].

ACKNOWLEDGMENTS

We thank J. Richter for insightful discussions and comments on a first draft of this paper. This work was in part supported by Deutsche Forschungsgemeinschaft via SFB 1143.

[1] H. Tasaki, From nagaoka's ferromagnetism to flat-band ferromagnetism and beyond: An introduction to ferromagnetism in the hubbard model, Prog. Theor. Phys. **99**, 489 (1998).

[2] O. Derzhko, J. Richter, and M. Maksymenko, Strongly correlated flat-band systems: The route from heisenberg spins to hubbard electrons, Int. J. Mod. Phys. B **29**, 1530007 (2015).

[3] D. Leykam, A. Andreanov, and S. Flach, Artificial flat band systems: From lattice models to experiments, Adv. Phys.: X **3**, 1473052 (2018).

[4] S. A. Parameswaran, R. Roy, and S. L. Sondhi, Fractional quantum hall physics in topological flat bands, C. R. Phys. **14**, 816 (2013).

[5] E. J. Bergholtz and Z. Liu, Topological flat band models and fractional chern insulators, Int. J. Mod. Phys. B **27**, 1330017 (2013).

[6] D. N. Sheng, Z.-C. Gu, K. Sun, and L. Sheng, Fractional quantum Hall effect in the absence of Landau levels, Nat. Commun. **2**, 389 (2011).

[7] Y.-F. Wang, Z.-C. Gu, C.-D. Gong, and D. N. Sheng, Fractional Quantum Hall Effect of Hard-Core Bosons in Topological Flat Bands, Phys. Rev. Lett. **107**, 146803 (2011).

[8] T. Neupert, L. Santos, C. Chamon, and C. Mudry, Fractional Quantum Hall States at Zero Magnetic Field, Phys. Rev. Lett. **106**, 236804 (2011).

[9] K. Sun, Z. Gu, H. Katsura, and S. Das Sarma, Nearly Flatbands with Nontrivial Topology, Phys. Rev. Lett. **106**, 236803 (2011).

[10] E. Tang, J.-W. Mei, and X.-G. Wen, High-Temperature Fractional Quantum Hall States, Phys. Rev. Lett. **106**, 236802 (2011).

[11] M. Imada and M. Kohno, Superconductivity from Flat Dispersion Designed in Doped Mott Insulators, Phys. Rev. Lett. **84**, 143 (2000).

[12] S. Peotta and P. Törmä, Superfluidity in topologically nontrivial flat bands, Nat. Commun. **6**, 8944 (2015).

[13] C. Wu, D. Bergman, L. Balents, and S. Das Sarma, Flat Bands and Wigner Crystallization in the Honeycomb Optical Lattice, Phys. Rev. Lett. **99**, 070401 (2007).

[14] B. Jaworowski, A. D. Güçlü, P. Kaczmarkiewicz, M. Kupczyński, P. Potasz, and A. Wójs, Wigner crystallization in topological flat bands, New J. Phys. **20**, 063023 (2018).

[15] B. Dóra, J. Kailasvuori, and R. Moessner, Lattice generalization of the Dirac equation to general spin and the role of the flat band, Phys. Rev. B **84**, 195422 (2011).

[16] A. Ramachandran, A. Andreanov, and S. Flach, Chiral flat bands: Existence, engineering, and stability, Phys. Rev. B **96**, 161104(R) (2017).

[17] S. D. Huber and E. Altman, Bose condensation in flat bands, Phys. Rev. B **82**, 184502 (2010).

[18] B. Pal and K. Saha, Flat bands in fractal-like geometry, Phys. Rev. B **97**, 195101 (2018).

[19] M. Maksymenko, R. Moessner, and K. Shtengel, Persistence of the flat band in a kagome magnet with dipolar interactions, Phys. Rev. B **96**, 134411 (2017).

[20] L. Du, X. Zhou, and G. A. Fiete, Quadratic band touching points and flat bands in two-dimensional topological Floquet systems, Phys. Rev. B **95**, 035136 (2017).

[21] P. Roman-Taboada and G. G. Naumis, Topological flat bands in time-periodically driven uniaxial strained graphene nanoribbons, Phys. Rev. B **95**, 115440 (2017).

[22] J. Schulenburg, A. Honecker, J. Schnack, J. Richter, and H.-J. Schmidt, Macroscopic Magnetization Jumps due to Independent Magnons in Frustrated Quantum Spin Lattices, Phys. Rev. Lett. **88**, 167207 (2002).
[23] M. E. Zhitomirsky and H. Tsunetsugu, High field properties of geometrically frustrated magnets, Prog. Theor. Phys. Suppl. **160**, 361 (2005).
[24] H.-J. Schmidt, J. Richter, and R. Moessner, Linear independence of localized magnon states, J. Phys. A **39**, 10673 (2006).
[25] O. Derzhko, J. Richter, A. Honecker, and H.-J. Schmidt, Universal properties of highly frustrated quantum magnets in strong magnetic fields, Low Temp. Phys. **33**, 745 (2007).
[26] J. T. Chalker, T. S. Pickles, and P. Shukla, Anderson localization in tight-binding models with flat bands, Phys. Rev. B **82**, 104209 (2010).
[27] S. Flach, D. Leykam, J. D. Bodyfelt, P. Matthies, and A. S. Desyatnikov, Detangling flat bands into fano lattices, Europhys. Lett. **105**, 30001 (2014).
[28] J. D. Bodyfelt, D. Leykam, C. Danieli, X. Yu, and S. Flach, Flatbands Under Correlated Perturbations, Phys. Rev. Lett. **113**, 236403 (2014).
[29] D. Leykam, J. D. Bodyfelt, A. S. Desyatnikov, and S. Flach, Localization of weakly disordered flat band states, Eur. Phys. J. B **90**, 1 (2017).
[30] N. Perchikov and O. V. Gendelman, Flat bands and compactons in mechanical lattices, Phys. Rev. E **96**, 052208 (2017).
[31] Y. Zong, S. Xia, L. Tang, D. Song, Y. Hu, Y. Pei, J. Su, Y. Li, and Z. Chen, Observation of localized flat-band states in kagome photonic lattices, Opt. Express **24**, 8877 (2016).
[32] D. Leykam and S. Flach, Perspective: Photonic flatbands, APL Photonics **3**, 070901 (2018).
[33] Z. Lin, J.-H. Choi, Q. Zhang, W. Qin, S. Yi, P. Wang, L. Li, Y. Wang, H. Zhang, Z. Sun, L. Wei, S. Zhang, T. Guo, Q. Lu, J.-H. Cho, C. Zeng, and Z. Zhang, Flatbands and Emergent Ferromagnetic Ordering in Fe_3Sn_2 Kagome Lattices, Phys. Rev. Lett. **121**, 096401 (2018).
[34] G.-B. Jo, J. Guzman, C. K. Thomas, P. Hosur, A. Vishwanath, and D. M. Stamper-Kurn, Ultracold Atoms in a Tunable Optical Kagome Lattice, Phys. Rev. Lett. **108**, 045305 (2012).
[35] A. Mielke, Ferromagnetic ground states for the Hubbard model on line graphs, J. Phys. A **24**, L73 (1991).
[36] A. Mielke, Ferromagnetism in the Hubbard model on line graphs and further considerations, J. Phys. A **24**, 3311 (1991).
[37] A. Mielke, Exact ground states for the Hubbard model on the Kagome lattice, J. Phys. A **25**, 4335 (1992).
[38] H. Tasaki, Ferromagnetism in the Hubbard Models with Degenerate Single-Electron Ground States, Phys. Rev. Lett. **69**, 1608 (1992).
[39] A. Mielke and H. Tasaki, Ferromagnetism in the Hubbard model. Examples from models with degenerate single-electron ground states, Commun. Math. Phys. **158**, 341 (1993).
[40] D. L. Bergman, C. Wu, and L. Balents, Band touching from real-space topology in frustrated hopping models, Phys. Rev. B **78**, 125104 (2008).
[41] K. Essafi, L. D. C. Jaubert, and M. Udagawa, Flat bands and dirac cones in breathing lattices, J. Phys.: Condens. Matter **29**, 315802 (2017).
[42] T. Bilitewski, M. E. Zhitomirsky, and R. Moessner, Jammed Spin Liquid in the Bond-Disordered Kagome Antiferromagnet, Phys. Rev. Lett. **119**, 247201 (2017).
[43] See Supplemental Material at http://link.aps.org/supplemental/10.1103/PhysRevB.98.235109 for additional details on the construction of the localised states and the derivation of the gap for translationally invariant models, which also includes Ref. [51].
[44] W. Maimaiti, A. Andreanov, H. C. Park, O. Gendelman, and S. Flach, Compact localized states and flat-band generators in one dimension, Phys. Rev. B **95**, 115135 (2017).
[45] W. Maimaiti, S. Flach, and A. Andreanov, Universal $d = 1$ flatband generator from compact localized states, arXiv:1810.08199.
[46] J.-W. Rhim and B.-J. Yang, Classification of flat bands from irremovable discontinuities of Bloch wave functions, arXiv:1808.05926.
[47] H. Tasaki, Stability of ferromagnetism in Hubbard models with nearly flat bands, J. Stat. Phys. **84**, 535 (1996).
[48] H. E. Stanley, Spherical model as the limit of infinite spin dimensionality, Phys. Rev. **176**, 718 (1968).
[49] D. A. Garanin and B. Canals, Classical spin liquid: Exact solution for the infinite-component antiferromagnetic model on the kagomé lattice, Phys. Rev. B **59**, 443 (1999).
[50] N. Read, Compactly supported Wannier functions and algebraic K-theory, Phys. Rev. B **95**, 115309 (2017).
[51] K. Roychowdhury, D. Zeb Rocklin, and M. J. Lawler, Topology and geometry of spin origami, Phys. Rev. Lett. **121**, 177201 (2018).